Published in final edited form as:
Sci Transl Med. 2014 February 26; 6(225): 225ra28. doi:10.1126/scitranslmed.3007607.

Wnt/β-catenin signaling in T-cells drives epigenetic imprinting of pro-inflammatory properties and promotes colitis and colon cancer

Shilpa Keerthivasan[1,†], **Katayoun Aghajani**[1,†], **Marei Dose**[1], **Luciana Molinero**[1], **Mohammad W. Khan**[2], **Vysak Venkatesvaran**[2], **Christopher Weber**[3], **Akinola Olumide Emmanuel**[1], **Tianjao Sun**[1], **Elena M. Ramos**[4], **Ali Keshavarzian**[5], **Mary Mulcahy**[6], **Nichole Blatner**[2], **Khashayarsha Khazaie**[2], and **Fotini Gounari**[1,*]

[1]Knapp Center for Lupus and Immunology Research, The University of Chicago, Chicago, IL, 60637, USA

[2]Robert H. Lurie Comprehensive Cancer Center, Northwestern University, Chicago, IL 60611, USA

[3]Department of Pathology, The University of Chicago, Chicago, IL, 60637, USA

[4]Pathology Core Facility, Robert H. Lurie Comprehensive Cancer Center, Northwestern University, Chicago, IL 60611, USA

[5]Division of Digestive Diseases and Nutrition, Department of Medicine, RUSH University Medical Center, Chicago, IL, 60612

[6]Department of Hematology/Oncology, Northwestern Medical Faculty Foundation, Chicago, IL 60611, USA

Abstract

The density and type of lymphocytes that infiltrate colon tumors are predictive of the clinical outcome of colon cancer. High densities of TH17 cells and inflammation predict poor outcome, while infiltration by Tregs that naturally suppress inflammation is associated with longer patient survival. However, the role of Tregs in cancer remains controversial. We recently reported that Tregs in colon cancer patients can become pro-inflammatory and tumor promoting. These properties were directly linked with their expression of RORγt, the signature transcription factor of TH17 cells. Here, we report that Wnt/β-catenin signaling in T-cells promotes expression of

*To whom correspondence should be addressed. fgounari@uchicago.edu.
†These authors contributed equally to the publication

Author contributions: K.A. designed and performed experiments and analyzed the data, S.K. designed and performed experiments and analyzed the data. M.D. performed the epigenetic studies. L.M. provided experimental expertise and analyzed data; C.W. analyzed histological samples; J.D.P., S.H., B.P.S., conducted experiments. A.O.E. performed epigenetic analyses; T.S. performed experiments; N.R.B. gave conceptual and technical advice and performed experiments; M.W.K. and V.V. performed immunostainings and analyzed data; ML consented patients acquired specimens and helped with preparation and analysis of blood; AK provided patient specimens and information and advice for analysis; K.K. gave conceptual and technical advice and helped with design of experiments and writing of the paper; F.G. designed the experiments, analyzed the data, and wrote the paper.

Competing interests: The authors declare that they have no competing interests.

Data and materials availability: The data generated by this study have been deposited in the Gene Expression Omnibus database (GSE41229 and GSE7050).

RORγt. Expression of β-catenin was elevated in T-cells and Tregs of patients with colitis and colon cancer. Genetically engineered activation of β-catenin in mouse T-cells resulted in enhanced chromatin accessibility in the proximity of Tcf-1 binding sites genome-wide, induced expression of TH17 signature genes including RORγt, and promoted TH17-mediated inflammation. Strikingly, the mice had inflammation of intestine and colon and developed lesions indistinguishable from colitis-induced cancer. Activation of β-catenin only in Tregs was sufficient to produce inflammation and initiate cancer. Based on these findings we conclude that activation of Wnt/β-catenin signaling in T-cells and/or Tregs is causatively linked with the imprinting of pro-inflammatory properties and the promotion of colon cancer.

Introduction

The gastrointestinal tract is poised in a state of equilibrium that permits rapid protective responses against pathogens but curtails damage by hindering long-lasting vigorous inflammatory processes. This balance is achieved through interactions between pro-inflammatory T-helper-17 (TH17) cells and anti-inflammatory regulatory T-cells (Tregs) (1) that suppress TH17 inflammation in an IL-10 dependent manner (2–5). Autoimmune disorders, in particular human inflammatory bowel disease (IBD), are etiologically associated with chronically deregulated inflammation (6, 7). Both the progression of IBD to cancer (8) and initiation and progression of sporadic colon cancer are driven by inflammation (9–12). Accordingly, infiltration of colon cancer tumors with TH17 cells negatively correlates with patient survival (13), while high densities of Tregs predict better clinical outcomes (13–15). The protective role of Tregs in colon cancer is, however, controversial and other reports suggest a negative correlation with high Treg densities and disease outcome (16). We reported earlier that in human colon cancer there is preferential expansion of a Treg subset that is potently T-cell suppressive but has TH17 characteristics (11, 12, 17–19). These Tregs express the signature TH17 transcription factor retinoic acid related orphan receptor-γt (ROR-γt) and promote inflammation and tumor growth (11, 12, 18). Expression of RORγt by T-cells and Tregs is pivotal for sustaining pathologic inflammation in mouse polyposis, and genetic ablation of RORγt in these cells protects against polyposis (12, 17). It is unclear what triggers upregulation of RORγt in T-cells in the course of polyposis and colon cancer. Elucidating the molecular mechanisms that shift the lymphocyte balance from anti-inflammatory to pro-inflammatory will improve diagnosis and treatment of IBD and colon cancer.

Inactivation of the adenomatous polyposis coli (APC) gene is the initiating event in approximately 80% of human colon cancer cases (20), inducing the development of aberrant crypt foci and polyps (21, 22). Polyp growth is directly linked with stabilization of β-catenin (22, 23), the central effector of the Wnt signaling pathway. Focal inflammatory reactions in response to the oncogenic event (22) and to the gut microbiota (24) also contribute to disease progression. In thymocytes, β-catenin is activated by T-cell receptor (TCR) signaling, and together with its T-cell specific DNA binding partner Tcf-1, β-catenin promotes thymic development and selection (25–30). The transgenic overexpression of β-catenin in thymocytes promotes expression of RORγt, which in turn controls the expression of pro-survival genes (31). Accordingly, enhanced β-catenin activity is suggested to promote

survival of *ex vivo* generated mouse Tregs (32). By contrast, more recent findings suggest that pharmacologic activation of Wnt signaling suppresses Foxp3 and compromises the function of *ex vivo* differentiated human Tregs (33). Furthermore, the *ex vivo* differentiation of TH17 cells coincides with upregulation of β-catenin and Wnt signaling genes (34), and ablation of Tcf-1 promotes expression of IL-17 by T-cells (35, 36). These findings are consistent with the notion that Wnt/β-catenin signaling promotes TH17 differentiation.

In the present study we evaluated the role of Wnt/β-catenin in dictating T-cell functions in colitis and colon cancer, and the pathogenic consequences thereof. We found that the expression of RORγt and gain of pro-inflammatory functions by T-cells and Tregs in colitis and colon cancer are regulated through β-catenin-mediated epigenetic reprograming. Through the combined use of mouse models and patient specimens we demonstrate the relevance of these findings to ulcerative colitis, Crohn's disease, and colon cancer in humans. These findings provide a mechanistic explanation for the chronic shift in lymphocyte properties from anti-inflammatory to pro-inflammatory and highlight the significant role of Wnt signaling by T-cells in the epigenetic imprinting of inflammation in autoimmunity and cancer.

Results

In human colitis and colon cancer, T-cells express elevated levels of β-catenin

Earlier we provided evidence that β-catenin can be activated downstream of the T-cell receptor (26). Both inflammatory bowel disease and colon cancer involve activation of T-cells; therefore, we investigated the possibility that the Wnt/β-catenin pathway was upregulated in T-cells in these diseases. We examined tumor sections from patients with long standing ulcerative colitis and colon cancer. Tumor sections and colitis samples were compared to non-inflamed, non-cancerous control colon tissue from patients with arteriovenous malformation (AVM) or diverticular disease. Colonic tissues were sectioned and stained with specific antibodies to CD3 (T-cells) and β-catenin and revealed by secondary fluorescent conjugated antibodies. Expression CD3 and β-catenin in the same cell was established by confocal microscopy.

We found that tumor tissues were enriched for lymphocytes exhibiting strong membrane as well as cytoplasmic co-expression of β-catenin and CD3 (Fig. 1 A, a and b). We quantified the frequencies of β-catenin expressing T-cells in non-cancerous colitis specimens (Fig. 1 A, c and d), healthy colon (Fig. 1 A, e and f), sporadic colon cancer tumors (Fig. 1 A, g and h), and healthy margin of sporadic tumor cancers (Fig. 1 A, i and j). Analysis of the recorded images established that significantly increased numbers of T-cells infiltrated tumors as compared to colitis tissue (Fig. 1 B **left panel)**. A significantly increased fraction of infiltrating T-cells in both colitis and tumor tissue showed expression of β-catenin compared to T-cells in healthy colon, or in the margins of tumors obtained from sporadic colon cancer patients (Fig. 1 B, **right panel**). To further relate these changes in the tumor to systemic immunity, we determined the expression levels of β-catenin in lysates of purified $CD4^+$ T-cells and $CD4^+CD25^+$ Tregs from peripheral blood of colon cancer patients. Western blot analysis showed that T cells from cancer patients, including both Tregs and non-Treg $CD4^+$ T-cells, had significantly higher levels of β-catenin compared to healthy donors (Fig. 1 C).

These findings suggest that T-cells upregulate expression of β-catenin in ulcerative colitis and in colon cancer.

TH17 and Wnt/β-catenin signature genes are upregulated in intestinal T-cells during polyposis

To determine whether β-catenin activity in T-cells contributes to inflammation and cancer, we investigated $APC^{+/\Delta 468}$ mice, which have a heterozygous deletion of the Adenomatous Polyposis Coli (APC) gene, and develop hereditary polyposis (22, 37, 38). Analysis of polyp-ridden mice at 3 months of age revealed high frequencies of activated T-cells in both spleen (50% activated versus 10% in healthy animals) and intestine (80% activated versus 50% in healthy animals) (Fig. 2 A, B). To measure expression of β-catenin, we sorted $CD4^+$ T-cells and $CD4^+Foxp3^+$ Tregs (>97% purity) from Foxp3-GFP reporter mice on the WT or $APC^{+/\Delta 468}$ background (Fig. S1 A). Lysates of the purified cells were analyzed by western blot. Gut infiltrating $CD4^+$ T-cells and Tregs had elevated levels of β-catenin as compared to spleen (SP) and mesenteric lymph nodes (MLN), and these levels increased during polyposis (Fig. 2 C, D; Fig. S1 B). To determine if β-catenin was stabilized in T-cells during polyposis in response to cell extrinsic stimuli and not because of the mutated APC allele, we targeted loss of APC to epithelial cells. To this end we crossed the conditional APC^{lox468} mice (39, 40) with Ts4Cre transgenic mice (41) that express Cre specifically in gut epithelial cells. We found elevated levels of β-catenin in T-cells derived from aged polyp-ridden $Ts4CreAPC^{+/lox468}$ mice (Fig. S2), strengthening our conclusion that stabilization of β-catenin in T-cells was cell extrinsic.

To determine how the tumor microenvironment affected gene expression in T-cells, we investigated the expression profiles of T-cells and Tregs during polyposis. RNA was prepared from $CD4^+$ T-cells and Tregs sorted to ~97% purity and interrogated by ImmGen using Affymetrix arrays (Fig. S1 A) (12). Expression of Wnt pathway genes was compared between polyp-ridden $APC^{+/\Delta 468}$ and WT mice by Gene Set Enrichment Analysis (GSEA, MIT) using a Wnt-pathway Gene set (KEGG_WNT_SIGNALING_PATHWAY). This analysis revealed significant ($p<0.001$) enrichment in the expression of Wnt pathway genes in $CD4^+$ T-cells infiltrating the intestine of $APC^{+/\Delta 468}$ mice (Fig. 2 E, F). A weaker but significant ($p=0.02$) enrichment of Wnt pathway genes was detected in Tregs infiltrating the intestinal tumors (Fig. S1 C). Furthermore, expression of multiple genes associated with the TH17 lineage, including IL-17 and RORγt, by intestine infiltrating T-cells was increased during polyposis (Fig. 2 G). This finding is in line with an earlier report that Wnt pathway genes are upregulated during *ex vivo* TH17 commitment (34), and with our earlier findings that $ROR\gamma t^+$ T-cells are more frequent in the intestine of polyp-ridden $APC^{+/\Delta 468}$ mice (12) and Ts4Cre $APC^{+/lox468}$ mice (38). Taken together, these observations connect Wnt/γ-catenin signaling with the gain of TH17 characteristics by T-cells and Tregs during polyposis.

Activation of β-catenin in T-cells predisposes mice to intestinal inflammation, colitis, and cancer

To understand the biological outcome of expression of β-catenin in T-cells, we activated β-catenin specifically in T-cells using CD4Cre (42) and $Ctnnb1^{ex3}$ mice (21). In the compound

mutant CD4Cre Ctnnb1^{ex3} mice, CD4Cre dependent excision of β-catenin exon-3 removes phosphorylation sites that target the protein for degradation, thereby producing stable, dominant, constitutively active β-catenin in T-cells and Tregs. The CD4CreCtnnb1^{ex3} (heterozygous Ctnnb1^{ex3} allele) compound mutant progeny developed cachexia and rectal prolapse as early as 8–10 weeks of age. Histologic analysis revealed crypt elongation in the colon and crypt and villus elongation in the small intestine as compared to littermate CD4Cre controls (Fig. 3 A). Accordingly, as early as 6 weeks of age epithelial cells in both the small intestine and colon of these mice had increased mitotic activity in comparison with healthy mice (Fig. 3 B, C). By 8–10 weeks of age, CD4CreCtnnb1^{ex3} mice began to develop small intestine inflammation and chronic colitis. We observed progressive leukocyte infiltration that promoted ulcers and crypt distortion (Fig. 3 D a, b), granulomas (Fig. 3 D c), and crypt abscesses (Fig. 3 D d), as well as invasive crypts (Fig. S3 A, B). The epithelial cells in the invasive crypts exhibited peripheral localization of β-catenin (Fig. S3 C, D) typical of reactive tissue. By 4–8 months of age, all mice had developed colitis and prolapses, and more than half (n=13) had developed from 1 to 3 polyps, which were identified morphologically and by nuclear β-catenin staining (Fig. S3 E, F). Polyps were concentrated in the distal ileum and proximal colon close to the caecum (Fig S4). Small intestine polyps were histologically indistinguishable from those detected in APC$^{+/\Delta 468}$ mice (Fig. 3 E, F), while colonic polyps had a serrated architecture (Fig. 3 G).

To determine the contribution of Wnt/β-catenin signaling in Tregs to colitis and cancer, we targeted stabilization of β-catenin to Tregs by crossing Ctnnb1^{ex3} mice (21) to Foxp3-Cre mice (5). A progressive inflammation leading to polyp formation was observed at four (n=3), six (n=3), and nine months (n=3) of age in compound mutant mice that expressed both genes. At four months the mice had enlarged lymphoid follicles in the small intestine underlying normal looking villi (Fig. S5 A). By six months of age follicle had become abnormally enlarged and covered by crypt and villus structures (Fig. S5 B), and by nine months follicles were very large underlying aberrant crypts (Fig. S5 C, D). Abnormally enlarged lymphoid follicles were also apparent in the colon (Fig. S5 E, F). Nine month old mice had hyperproliferative and aberrant crypts as well as adenomatous polyps (Fig. 3 H, J). These findings highlight the importance of β-catenin activation in Tregs for the gut inflammation and polyposis.

Polyps in the small intestine and colon were densely infiltrated with mast cells, which localized to the parenchyma, stroma, and submucosa of the lesions (Fig. S6 A, B). Mastocytosis was focal, and mast cell numbers declined outside the polyps (Fig. S6 C). CD11b^{+} myeloid cells, B220^{+} B-cells, and CD11c^{+} antigen presenting cells were increased in numbers in the spleen and lymph nodes of the mice, indicating both local and systemic inflammation (Fig. S6 D).

Constitutive activation of β-catenin in T-cells promotes TH-17 commitment and sustained inflammation

To confirm that gut pathologies were induced by constitutive activation of β-catenin in T-cells rather than by leaky expression of Cre in gut epithelial cells, we depleted T-cells and B-cells by introducing a homozygous Rag2 mutation in CD4CreCtnnb1^{ex3} mice.

CD4CreCtnnb1^{ex3} Rag2$^{-/-}$ mice (n=10) observed until 10 months of age did not exhibit inflammation or polyps (Fig. 4 A), demonstrating that progressive colitis and growth of polyps in CD4CreCtnnb1^{ex3} mice were strictly lymphocyte dependent. Additionally, intracellular β-catenin staining and FACS analysis of leukocytes derived from CD4CreCtnnb1^{ex3} mice revealed that β-catenin protein levels were elevated in circulating CD4 and CD8 T-cells but not in macrophages, dendritic cells, or B-cells (Fig. 4 B). Stabilization of β-catenin was validated by western blot (WB) analysis of sorted CD4^{+} T-cells, which showed elevated levels of β-catenin in CD4^{+} T-cells from the spleen, and small intestine (Fig. 4 C).

To investigate the mechanism of action of β-catenin in T-cells, we determined their activation status and numbers. T-cells with constitutively active β-catenin expressed several activation markers including CD69, CD122, and NKG2D, and they down-regulated CD62L (Fig. 4 D). We reported earlier that stabilization of β-catenin during thymic development stalls differentiation of T-cells at the DP stage (26, 27). Accordingly, at 4 weeks of age CD4CreCtnnb1^{ex3} mice had fewer thymic and peripheral CD4^{+} and CD8^{+} T-cells; however, by 8 weeks of age the absolute numbers of peripheral T-cells had increased to near normal levels (Fig. 4 E).

An abnormally large fraction of CD4^{+} T-cells from CD4CreCtnnb1^{ex3} mice expressed IL-17 in the thymus as well as in peripheral lymphoid organs including mesenteric lymph nodes and intestine as compared to WT mice (Fig. 5 A, B). Furthermore, pro-inflammatory cytokines IL-17, TNFα, and IL6 were elevated in the small intestine and caecum of CD4CreCtnnb1^{ex3} mice (Fig. 5 C). To validate these findings, we transferred total peripheral T-cells (10^{6} cells/mouse) from CD4CreCtnnb1^{ex3} or control CD4Cre mice to Rag2$^{-/-}$ recipients. Three weeks after transfer, TH17 and TH1 cytokines, as well as IL-10 but not IL-2, were significantly higher in the serum of mice that received T-cells with constitutively active β-catenin (CD4CreCtnnb1^{ex3}) as compared to mice that received control T-cells (CD4Cre) (Fig. 5 D). Mice receiving CD4CreCtnnb1^{ex3} T-cells did not survive beyond four weeks after transfer, while those receiving CD4Cre T-cells remained viable. These observations demonstrate that T-cells with elevated levels of β-catenin are TH17 biased and proinflammatory. This is in line with an earlier report that β-catenin is upregulated in *ex vivo* differentiated TH17 cells (34). Based on these observations we conclude that high levels of β-catenin in T-cells causes chronic T-cell activation, TH17 commitment, and pathogenic inflammation that predisposes the small intestine and colon to cancer.

Activation of β-catenin impairs normal Treg development and function

Expression of β-catenin enhances survival of *ex vivo* differentiated Tregs (32), raising the possibility that constitutive activation of β-catenin may lead to Treg expansion. We observed that reduced numbers of thymic Foxp3^{+}CD4^{+} Tregs were generated in CD4CreCtnnb1^{ex3} mice as compared to controls (Fig 6 A). However, a similar reduction was not apparent in spleen and lymph nodes (Fig 6 A), suggesting a developmental defect that is compensated in the periphery, perhaps through generation and/or survival of extra-thymic Tregs. To confirm that the defect was cell intrinsic, we generated competitive bone

marrow chimeras in which BM progenitors from CD4CreCtnnb1^{ex3} mice (Thy1.2) and WT (Thy1.1) BM progenitors were mixed 1:1 and injected into lethally irradiated syngeneic WT hosts. Assessed 6 weeks after transfer, CD4CreCtnnb1^{ex3} BM progenitors gave rise to significantly fewer thymic Tregs than did WT BM progenitors (Fig. S7). Based on this, we conclude that the reduced frequencies of thymic Tregs in CD4CreCtnnb1^{ex3} mice resulted from a cell intrinsic defect.

Normally, Tregs have potent anti-inflammatory properties. Adoptive transfer of Tregs from healthy mice to lymphopenic mice suppresses the cytokine storm caused by prior or simultaneous transfer of naive CD4 T-cells (43). The ability of Tregs to suppress inflammation is protective, and similar adoptive transfers into polyp-ridden mice suppress cancer associated inflammation and cause regression of the polyps (18). However, we previously showed that Tregs from mice with polyposis (18) or from colon cancer patients are functionally altered (12, 44), exhibit TH17 characteristics, and promote inflammation and tumor growth. Therefore, we considered the possibility that Tregs with stabilized β-catenin may have lost their anti-inflammatory functions, and that this impairment is an underlying mechanism in colitis and colon cancer.

To evaluate this possibility we first induced colitis by transfer of naïve CD4$^+$ T-cells (CD4$^+$CD45^{RBhi}CD25$^-$ Thy1.1) into Rag2$^{-/-}$ mice. Four weeks later, when the mice started losing weight, we transferred CD4CreCtnnb1^{ex3} or CD4Cre Tregs (CD4$^+$CD25^{hi} or CD4$^+$Foxp3-GFP$^+$ Thy1.2$^+$) to suppress the colitis. Tregs with constitutively active β-catenin were significantly less effective than control (CD4Cre) Tregs in protecting the recipient mice from colitis (Fig. 6 B, C; Fig. S8). Analysis of Thy1.2$^+$CD4$^+$Foxp3-GFP$^+$ Tregs retrieved from the colon of Rag2$^{-/-}$ recipients at the end point showed that a significantly larger fraction of the transferred Tregs with constitutively active β-catenin expressed pro-inflammatory cytokines including IL-17, IFNγ, and TNFα as compared to transferred WT Tregs (Fig. 6 D, E). Tregs are also potent suppressors of T-cell functions, which normally is assayed by their ability to suppress proliferation of stimulated CD4$^+$ T-cells *in vitro*. Foxp3$^+$ Tregs with constitutively active β-catenin inhibited proliferation of CD4$^+$ T-cells although with less potency than control CD4Cre Tregs (Fig. 6 F). These observations demonstrate that activation of β-catenin in Tregs impairs their anti-inflammatory functions and contributes to systemic inflammation, colitis, and polyposis in CD4CreCtnnb1^{ex3} mice.

β-catenin increases chromatin accessibility and expression of target genes

To gain insight into the molecular mechanisms by which β-catenin alters the properties of T-cells, we compared gene expression of CD4CreCtnnb1^{ex3} and WT thymocytes using Affymetrix arrays (27). T-cell specific activation of β-catenin resulted in robust expression of TH17 family genes including RORγt, the signature transcription factor of the TH17 lineage, in CD4CreCtnnb1^{ex3} thymocytes (Fig. 7 A). This expression pattern showed significant overlap with that of T-cells from polyp-ridden APC$^{+/\Delta 468}$ mice (Fig. 2 G). To investigate the underlying reason for the change in gene expression, we performed ChIP-Seq analyses of Tcf-1 combined with mapping of histone marks. In WT thymocytes, Tcf-1 preferentially bound to consensus TCF motifs ($p<10^{-940}$) within enhancers and promoters,

and displayed genome wide association with marks of open chromatin such as lysine acetylation of histone-3 (H3KAc) (Fig. 7 B, upper panels, black lines). In contrast, there was little association of Tcf-1 with marks of closed chromatin such as lysine 27 tri-methylation of histone-3 (H3K27me3) (Fig. 7 B, lower panels, black lines). Stabilization of β-catenin in CD4CreCtnnb1^{ex3} thymocytes significantly enhanced H3KAc marks in both promoters and enhancers spanning more than 3 kb from the Tcf-1 binding sites (Fig. 7 B, upper panels, red lines). Conversely, H3K27me3 marks (Fig. 7 B, lower panels, red lines) were reduced. These observations are consistent with the notion that the observed activation of gene expression involves interaction of β-catenin with its T-cell specific DNA binding partner Tcf-1. Presumably, Tcf-1 binds accessible loci, and β-catenin enhances their accessibility. Therefore, we tested the possibility that enhanced accessibility could translate into elevated gene expression.

Given that RORγt is the signature transcription factor for TH17 differentiation and was found by our expression arrays to be upregulated in CD4CreCtnnb1^{ex3} thymocytes, we examined the epigenetic state of the Rorc locus, which encodes RORγt. Our ChIP-seq analysis revealed comparable Tcf-1 binding to *bona fide* promoter and intragenic regions of the RORγt gene in WT and CD4CreCtnnb1^{ex3} thymocytes (Fig. 7 C). Marks of open chromatin such as H3KAc were significantly elevated in the Tcf-1 bound regions (Fig. 7 C), covering a large part of the Rorc locus. This finding is in line with earlier findings that β-catenin induces histone acetylation by recruiting the histone acetyltransferases (HATs), CBP (cyclic AMP response element-binding protein), and p300 to Tcf sites (45).

Next, we tested RORγt expression using a transgenic RORγt reporter in T-cells that had constitutively activated β-catenin. We also performed intracellular staining for RORγt and RT-PCR. We crossed reporter mice that contained an insertion of the green fluorescent protein (G) gene in the RORγt gene (46) with CD4CreCtnnb1^{ex3}, WT, and CD4Cre mice. The resulting heterozygous RORγt$^{+/G}$ mice had one WT (+) and one truncated (G) RORγt allele, but were healthy with no detectable hematopoietic abnormalities or other pathologies. RORγt has an important role during thymic development but its expression is shut down at the CD4 SP stage. Accordingly, expression of the transgenic reporter was not detected in CD4$^+$ SP thymocytes of WT or CD4Cre. However, significant expression was seen in CD4CreCtnnb1^{ex3} CD4$^+$ SP thymocytes that had stabilized β-catenin (Fig. 7 D). CD4CreCtnnb1^{ex3} CD4$^+$ SP thymocytes exhibited significant RORγt expression in peripheral CD4 T-cells (~8%) and in Tregs (~7%) (Fig. 7 E). Consistently, levels of RORγt expression were found to be approximately 5-fold higher in thymic and peripheral Tregs with stabilized β-catenin (Fig. S9). Thus, by three different assays, increased expression of RORγt was seen in thymocytes and T-cells that had constitutively active β-catenin.

These findings demonstrate that activation of β-catenin in T-cells introduces global changes in the chromatin landscape, increases accessibility, and enhances expression of target genes including RORγt.

RORγt functions downstream of β-catenin to compromise Treg properties

RORγt is the signature transcription factor of TH17 cells raising the possibility that the T-cell abnormalities produced by constitutive activation of β-catenin are in part caused by

deregulated expression of RORγt. Therefore, we analyzed CD4CreCtnnb1^{ex3} mice that cannot express RORγt because they are homozygous for the RORγt$^{G/G}$ allele but have constitutively activated β-catenin. In the absence of RORγt normal development and function of T-cells and Tregs were partially restored despite the presence of constitutively active β-catenin. In particular, ablation of RORγt reduced the frequencies of IL-17 expressing peripheral CD4^{+} T-cells and Tregs to levels comparable to WT (Fig. 8 A). This confirmed that RORγt was indispensable in deregulation of TH17 inflammation by β-catenin. Ablation of RORγt also increased the frequency of thymic Tregs (Fig. 8 B) and restored the expression Foxp3 protein to normal levels (Fig. 8 C). Importantly, ablation of RORγt in CD4CreCtnnb1^{ex3} Tregs with constitutively active β-catenin significantly improved their ability to suppress proliferation of *in vitro* activated T-cells (Fig. 8 E). These findings are consistent with the interpretation that Treg dysfunction in CD4CreCtnnb1^{ex3} mice is the result of persistent β-catenin activity and activation of RORγt.

Discussion

In a recent analysis of human colon cancer and mouse polyposis, we observed the preferential expansion of a subset of Tregs that co-express Foxp3 and RORγt and are potently T-cell suppressive but promote inflammation (12). RORγt is the signature transcription factor of TH17 cells, and is also upregulated in T-cells in association with inflammatory events during colon cancer. In the current study we observed that expression of β-catenin was significantly increased in colon infiltrating T-cells of patients with long lasting ulcerative colitis. The frequencies of these cells increased as the chronically inflamed tissues progressed to cancer, and was highest inside the tumors. T-cells are activated in response to inflammation and cancer, and accordingly, we observed significant expression of β-catenin in circulating T-cells and Tregs of colon cancer patients. These findings led us to question a mechanistic link between the expression of β-catenin and the expression of RORγt in T-cells during colitis and colon cancer (12).

The biological significance of β-catenin activation in T-cells was revealed by analysis of mouse models. Previously, we had shown that APC$^{+/\Delta 468}$ mice with hereditary polyposis depend on TH17 cytokines to develop polyps, and in addition, have a significant subset of RORγt^{+} Tregs with pro-inflammatory properties. This model allowed us to examine how expression of RORγt was related to expression of β-catenin. We demonstrated by independent assays (western blot and expression array analysis) that in polyp-ridden APC$^{+/\Delta 468}$ mice effector T-cells and Tregs express high levels of β-catenin and Wnt pathway genes. To directly test the biological impact of sustained β-catenin activity we used the CD4CreCtnnb1^{ex3} mouse model in which CD4Cre-mediated deletion of the degradation domain of the endogenous β-catenin stabilizes the protein only in T-cells. Using this model, we showed that persistent Wnt/β-catenin signaling in T-cells culminated in long lasting colitis, eventually progressing to intestinal and colon cancer. We ruled out the possibility that this pathology resulted from leaky expression of stable β-catenin in gut epithelial cells, by showing absence of disease in the lymphocyte deficient Rag2$^{-/-}$ CD4CreCtnnb1^{ex3} mice. It is well known that chronic inflammation in the colon predisposes to cancer, and our mouse models provided new insights into the mechanistic relevance of β-catenin signaling in T-cells to this process. In particular, the mouse model demonstrated that sustained

activation of β-catenin in human T-cells is biologically significant. This is shown by the facts that mice with polyposis had similar T-cell profiles as human patients, and targeted stabilization of β-catenin in mice with no APC mutation produced progressive inflammation and cancer in both the small intestine and colon.

Our earlier studies highlighted the strategically important role of Tregs in control of TH17 inflammation during mouse polyposis (18), and also pointed to a similar function in human colon cancer (12). We previously showed that Treg-targeted ablation of RORγt protects $APC^{+/\Delta 468}$ mice against polyposis. Here we demonstrated that Treg-targeted activation of β-catenin increased gut infiltration by lymphocytes and culminated in reactive tissue as well as bona fide adenomatous polyps. These observations are in agreement with the notion that Wnt/β-catenin signaling in Tregs is critical for gain of Treg pro-inflammatory properties and contributes to the carcinogenic processes in the intestine and colon.

Stabilized β-catenin mediates its effects by translocating to the nucleus, where it interacts with DNA binding TCF/Lef factors and regulates transcription of target genes. We showed that expression of genes associated with T-cell activation and TH17 lineage commitment is upregulated immediately following stabilization of β-catenin in $CD4CreCtnnb1^{ex3}$ thymocytes. Many of these genes were naturally elevated in gut infiltrating T-cells during polyposis. These global changes in gene expression involved β-catenin-induced changes in chromatin accessibility. ChIP-seq of Tcf-1 and chromatin marks revealed that in thymocytes Tcf-1 binds primarily to its conserved binding motifs in *bona fide* promoter and enhancer regions of target genes. Activation of β-catenin increased the accessibility of these sites through the deposition of H3KAc marks over long distances from the Tcf-1 binding. Our results are consistent with earlier findings in drosophila showing recruitment of β-catenin to TCF DNA binding sites in complex with the histone H3 acetyltransferase (HAT) CBP, and rapid, extensive histone acetylation (47).

We showed that Tcf-1 binds to consensus motifs in the Rorc locus, and activation of β-catenin enhances H3KAc in this locus as well as expression of RORγt in T-cells and Tregs. Our findings validate and extend recent observations that in double positive thymocytes RORγt gene expression is regulated by Wnt/β-catenin signaling (31). However, we did not find increased Tcf-1 binding to DNA in response to stabilization of β-catenin; rather, we observed that β-catenin enhances accessibility of the locus. Our findings are consistent with the fact that Wnt/β-catenin genes are upregulated during *in vitro* TH17 differentiation of T-cells (34). Our results are also consistent with reports that Tcf-1 suppresses IL-17 gene expression, and with the notion that elevated levels of β-catenin convert this suppression to activation (35, 36). Finally, our results are in agreement with a recent report indicating that Treg differentiation involves the programmed epigenetic closing of sequences with TCF/Lef binding motifs (48), and further suggest that elevated levels of β-catenin prevent this process resulting in TH17 commitment of thymocytes and defective Treg development.

In summary, we demonstrated that T-cells and Tregs have tumor-promoting roles in colon cancer that are epigenetically imprinted by Wnt/β-catenin signaling, the same pathway that initiates colon cancer in intestinal epithelial cells. In addition to T-cells, increased β-catenin activity has been also reported in pro-inflammatory monocytes and antigen presenting cells,

which could be part of a cancer field effect (49). In effect, our findings demonstrate that Wnt/β-catenin signaling unifies cancer-promoting events in the tumor as well as in the tumor environment. These findings are in line with the concept of a cancer landscape in which cells that surround solid tumors acquire epigenetic changes and alterations in gene expression that may be characteristic of the tumor itself (50).

Materials and Methods

Blood and tumor specimens

IRB protocols were approved by the Scientific Review Committee of Northwestern University, and informed consent was obtained from all participants. All patients had histologic diagnosis of Colon Cancer and had not received any prior therapy. Patients were tested for microsatellite instability (MSI: MLHa, MutL, and MutS), and patients testing positive were excluded. PB samples were drawn before surgical removal of the tumor. Total $CD3^+$ cells were isolated using the Dynabeads® Untouched™ Human CD4 T Cells - Life Technologies kit, and Tregs were then isolated using the CD4 CD25 regulatory T cell isolation kit, human (Miltenyi) by negative selection; purity was checked by flow cytometry. Paraffin embedded specimens of normal, non-inflamed colon from surgical specimens of 4 ulcerative colitis patients with active colitis and invasive colorectal cancer (cancer group) were obtained from Rush University Medical Center, Chicago. Additionally, surgical specimens from 7 patients who had surgery for non-malignant lesions such as colonic AVM or diverticular disease were used as controls [normal group]. All procedures were approved by the Rush University Medical Center Institutional Review Boards.

Mice

We previously reported mouse models of constitutive (18, 22, 37) and conditional (38, 39) truncation of exons 11 and 12 of the APC gene ($APC^{+/\Delta 468}$ and APC^{lox468}, respectively). TS4-Cre (41), $Ctnnb1^{ex3}$ (21), CD4Cre (42), and Foxp3Cre (5) mice were reported previously. C57BL/6J, $Rag2^{-/-}$, and $ROR\gamma t^{G/G}$ (B6.129P2(Cg)-$Rorc^{tm2Litt}$/J) mice were purchased from the Jackson laboratories. Mice were maintained under pathogen-free conditions, and investigated under the University of Chicago guidelines.

Flow cytometry and antibodies

Fluorescently labeled antibodies listed in Supplemental Table 1 were purchased from eBioscience and BD Pharmingen. Cell suspensions from thymus, spleen, MLN, and gut were stained in FACS buffer (2% fetal bovine serum in PBS) for 30 minutes on ice. Samples were washed with FACS buffer. Data were acquired with an LSRII flow-cytometer (Becton Dickinson) and analyzed using FlowJo software (TreeStar). Intracellular FoxP3 and RORγt staining was performed using the "Foxp3/ Transcription Factor Staining Buffer Set" (eBioscience). For intracellular cytokine staining, cells were stimulated with 50 ng/ml phorbol 12-myristate 13-acetate (PMA) (Sigma), 1 μM ionomycin (Sigma), and GolgiStop (BD Pharmingen) for 4 hours. After stimulation, cells were fixed and permeabilized and stained with antibodies against IFNγ, IL-17, TNFα, and IL-2 (eBioscience).

Histochemistry and Immunostaining

Paraffin sections (4 μM) were deparaffinized and stained with Hematoxylin and Eosin. For immunostaining, sections were deparaffinized in xylene, re-hydrated in a decreasing ethanol gradient, and antigen-retrieval was performed using a de-cloaking chamber at 120°C for 30 seconds and 90°C for 10 seconds in Dako target-retrieval solution followed by blocking with 5% goat serum. To stain mouse sections, rabbit anti-mouse β-catenin antibody (Santa Cruz Biotechnology) (1:100 dilution) was used overnight at 4°C. Antibody binding was revealed by HRP anti-rabbit secondary antibodies (1 hour at room temperature) and counterstained using Gill's II hematoxylin. Human specimens were stained with mouse anti-Human β-catenin (BD Biosciences) and Rabbit anti-Human CD3 (Neomarkers), or Mouse IgG1 (Abcam) and Rabbit IgG (Abcam) overnight (in Dako antibody-diluent) at 4°C. Sections were then washed 2X with Dako wash buffer for 5 minutes each and incubated with anti-Mouse Alexa Fluor 660 and anti-Rabbit Alexa Fluor 488 (secondary antibodies) for 1 hour at room temperature in the dark. Sections were washed 2X with Dako wash buffer 5 minutes each, stained with DAPI for 10 min, and then washed in PBS and mounted using Gelvatol. Sections were imaged using confocal microscopy (Leica). Images were recorded using the automated TissueGnostic method, and quantified by ImageJ in an unbiased manner.

Tissue lysates and multiplex ELISA

Portions of intestinal tissue as indicated in Results were dissected and homogenized in 1 ml phosphate buffered saline and centrifuged for 20 min at 4°C. Supernatant was collected, filtered (0.22 μM), and protein concentration was estimated using a Bradford assay. Multiplex ELISA and quantification of cytokines was conducted according to the manufacturer's instructions (Millipore). Plates were read in a Luminex 100 instrument and analyzed with xPONENT software (Luminex Corporation).

Mast Cell staining

To reveal mast cells, paraffin sections were stained with chloroacetate esterase (CAE) as described (12). Briefly, sections were stained for 20 min with CAE (naphthol-AS-D chloroacetate; Sigma) and counterstained for 3 min with hematoxylin Gill's II and 10% Toluidine Blue (Sigma).

BrdU staining

Mice were injected intraperitoneally with bromodeoxyuridine (BrdU; BD Pharmingen) (100 mg/kg) 2.5 h prior to euthanasia. The intestine was isolated, formalin fixed, jelly-rolled, and paraffin embedded. Tissue sections were deparaffinized using BD™ Retrievagen A and stained with anti-BrdU antibody according to the manufacturer's instructions (BD Biosciences).

Competitive BM chimeras

Lethally irradiated (950 rad; Gammacell 40) Thy1.1^{+} syngeneic mice (host) were injected with a 1:1 mixture of CD4CreCtnnb1^{ex3} (Thy1.2^{+}) and WT (Thy1.1^{+}) BM progenitors. Cells for the transfer were isolated by FACS-sorting for lack of surface expression of B220,

CD3, CD8, CD4, CD11b, CD11c, CD19, NK1.1, and Ter119 mature lineage markers. 1×10^6 BM progenitors were injected per mouse. Injected hosts were treated with Bactrim (trimethoprim/sulfamethoxazole) in the drinking water for the entire time of observation (6 weeks).

In vitro T-cell proliferation inhibition assay

Sorted $CD4^+CD44^{lo}CD25^-$ (CD45.1) naïve T cells (5×10^4 cells/well) were labeled with CFSE or cell proliferation dye eFluor 670 (eBioscience) according to the manufacturer's instructions. Labeled naïve T cells were stimulated with soluble anti CD3 (1 μg/ml; 2C11) in the presence of irradiated syngeneic splenocytes (2×10^5 cells/well). The cultures were supplemented with increasing numbers of independently sorted $CD4^+CD25^+$ or $CD4^+$ Foxp3-GFP^+ (CD45.2) Tregs (>95% purity). Cells were cultured for 72 hours, then stained for CD4 and CD45.1 expression, and analyzed by flow cytometry.

Induction of colitis

Sorted naive T cells ($CD4^+CD25^-CD45RB^{hi}$, 4×10^5) were transferred into $Rag2^{-/-}$ mice, which were weighed weekly to detect signs of wasting. After 4 weeks, Tregs ($CD4^+CD25^{hi}$, or $CD4^+$Foxp3-GFP^+ cells 1×10^5) were injected into the same recipients intravenously. Mice were euthanized 4 weeks after Treg transfer, and colons were analyzed histopathologically or used to prepare MNCs for analysis of cytokine expression. In alternative experiments, mice were injected simultaneously with naïve T cells (4×10^5) and Tregs (2×10^5).

Assessment of colitis

Colons were harvested from mice, flushed free of feces, and jelly-rolled for formalin fixation and paraffin embedding. Sections (4 μm) were used for H&E staining. Histologic assessment was performed in a blinded fashion using a scoring system previously described (51). Briefly, a numerical scale was used to denote the severity of inflammation (0, none; 1, mild; 2, moderate; and 3, severe), the level of involvement (0, none; 1, mucosa; 2, mucosa and submucosa; and 3, transmural), and extent of epithelial/crypt damage (0, none; 1, basal 1/3; 2, basal 2/3; 3, crypt loss; 4, crypt and surface epithelial destruction). Each variable was then multiplied by a factor reflecting the percentage of the colon involved (1, 0–25%; 2, 26–50%; 3, 51–75%; and 4, 76–100%); scores for severity, involvement, and damage were then summed to obtain the overall score.

Western blot

Lysates were prepared from cells isolated as indicated using RIPA buffer (20 mM TrisHcl pH7.5, 100 mM NaCl, 1 mM EDTA, 1% Triton x-100, 0.5% deoxycholic acid, 0.1% SDS) supplemented with protease inhibitors (Roche diagnostics). Lysates were electrophoresed and blotted, and the membrane was probed with antibodies against β-catenin (BD Biosciences) and β-tubulin (Thermo Fisher).

Real time PCR

Tregs were sorted as indicated and stimulated with PMA and ionomycin for 2 hrs. RNA was extracted using the RNeasy Mini kit (Qiagen). The RNA was DNAse treated, and cDNA was synthesized using SuperScript III (Invitrogen). Quantitative real time PCR was performed using actin as a normalizing control. The primer sequences used were: RORγt F2: TGCAAGACTCATCGACAAGG, RORγt R2: AGGGGATTCAACATCAGTGC (178 nt); IL-17 F: TCCAGAAGGCCCTCAGACTA, IL-17 R: AGCATCTTCTCGACCCTGAA (239 nt).

Gene Expression analysis

Cells were purified from the respective organs of male FoxP3-GFP and FoxP3-GFP $APC^{+/\Delta 468}$ reporter mice, enriched for $CD4^+$ T-cells, and then twice sorted to >97% purity (Fig S1 C). RNA was prepared according to protocols from the ImmGen consortium and submitted to ImmGen for microarray analysis following consortium procedures (http://immgen.org). A Gene Pattern Expression Dataset file was generated from genes associated with the TH17 lineage. Gene Set Enrichment Analysis (GSEA) of the Wnt pathway gene set (Biocarta) was performed using GSEA v2.08 (Broad Institute). Where indicated, replicates of each sample were grouped to calculate and cluster class means. Microarray data are available from NCBI under accession numbers GSE41229, and GSE7050.

Chromatin immunoprecipitation Sequence (ChIP-Seq)

ChIP–seq was performed as described (52). Briefly 10^7–10^8 total thymocytes from 4-week old mice were formaldehyde-fixed and sonicated to an average size of 300 bp. Antibodies recognizing Tcf-1 (53) (a kind gift of Hiroshi Kawamoto) coupled to Protein G Dynabeads were incubated overnight with sheared chromatin. ChIP-seq libraries were prepared from 10 ng of immunoprecipitated material as before (52) and sequenced on an Illumina Genome Analyzer 2. Data were analyzed as described (52). Briefly, reads were aligned to the mouse genome (mm9) using bowtie (54) allowing no mismatches. Peaks were called with MACS at a p-value cutoff of 10e-5 (55). Tcf-1 peaks were highly enriched for Tcf-1 binding motifs ($p<10e-940$). We have previously described ChIP-seq for H3K4me3 and H3K27me3 in WT thymocytes (52). Accession number for Tcf-1 ChIP-seq is GSE46662.

Supplementary Material

Refer to Web version on PubMed Central for supplementary material.

Acknowledgments

We thank Dr. Christoph Benoist for his continuous interest in this work, and for his guidance and encouragement; we thank Dr. Maria Louis Alegre for suggestions and comments on the manuscript. We are grateful to Dr. Abdulrahman Saadalla and Dr. Zahra Mojtahedi for help with processing patient specimens and isolating human T-cells.

Funding: This work was supported by National Institutes of Health Grant R21AI076720, P30 DK42086 pilot, and American Cancer Society Grant ACS/RSG, LIB-113428, (to F.G), NIH grant 1R01CA160436 and Circle of Service award (Robert H. Lurie Comprehensive Cancer Center, to K.K.). S.K. was supported by T325T32HL007381 Cardiovascular Sciences Training Grant.

References

1. Littman DR, Rudensky AY. Th17 and regulatory T cells in mediating and restraining inflammation. Cell. Mar 19.2010 140:845. [PubMed: 20303875]
2. Asseman C, Mauze S, Leach MW, Coffman RL, Powrie F. An essential role for interleukin 10 in the function of regulatory T cells that inhibit intestinal inflammation. J Exp Med. Oct 4.1999 190:995. [PubMed: 10510089]
3. Huber S, et al. Th17 cells express interleukin-10 receptor and are controlled by Foxp3 and Foxp3+ regulatory CD4+ T cells in an interleukin-10-dependent manner. Immunity. Apr 22.2011 34:554. [PubMed: 21511184]
4. Chaudhry A, et al. Interleukin-10 signaling in regulatory T cells is required for suppression of th17 cell-mediated inflammation. Immunity. Apr 22.2011 34:566. [PubMed: 21511185]
5. Rubtsov YP, et al. Regulatory T cell-derived interleukin-10 limits inflammation at environmental interfaces. Immunity. Apr.2008 28:546. [PubMed: 18387831]
6. Korn T, Bettelli E, Oukka M, Kuchroo VK. IL-17 and Th17 Cells. Annual review of immunology. 2009; 27:485.
7. Van Limbergen J, Wilson DC, Satsangi J. The genetics of Crohn's disease. Annual review of genomics and human genetics. 2009; 10:89.
8. Khan MW, et al. PI3K/AKT signaling is essential for communication between tissue-infiltrating mast cells, macrophages, and epithelial cells in colitis-induced cancer. Clin Cancer Res. May 1.2013 19:2342. [PubMed: 23487439]
9. Terzic J, Grivennikov S, Karin E, Karin M. Inflammation and colon cancer. Gastroenterology. Jun. 2010 138:2101. [PubMed: 20420949]
10. Khazaie K, et al. The significant role of mast cells in cancer. Cancer Metastasis Rev. Mar.2011 30:45. [PubMed: 21287360]
11. Blatner NR, et al. In colorectal cancer mast cells contribute to systemic regulatory T-cell dysfunction. Proc Natl Acad Sci U S A. Apr 6.2010 107:6430. [PubMed: 20308560]
12. Blatner NR, et al. Expression of RORgammat marks a pathogenic regulatory T cell subset in human colon cancer. Science translational medicine. Dec 12.2012 4:164ra159.
13. Tosolini M, et al. Clinical impact of different classes of infiltrating T cytotoxic and helper cells (Th1, th2, treg, th17) in patients with colorectal cancer. Cancer Res. Feb 15.2011 71:1263. [PubMed: 21303976]
14. Salama P, et al. Tumor-infiltrating FOXP3+ T regulatory cells show strong prognostic significance in colorectal cancer. J Clin Oncol. Jan 10.2009 27:186. [PubMed: 19064967]
15. Correale P, et al. Regulatory (FoxP3+) T-cell tumor infiltration is a favorable prognostic factor in advanced colon cancer patients undergoing chemo or chemoimmunotherapy. J Immunother. May. 2010 33:435. [PubMed: 20386463]
16. Sinicrope FA, et al. Intraepithelial effector (CD3+)/regulatory (FoxP3+) T-cell ratio predicts a clinical outcome of human colon carcinoma. Gastroenterology. Oct.2009 137:1270. [PubMed: 19577568]
17. Bos PD, Rudensky AY. Treg cells in cancer: a case of multiple personality disorder. Sci Transl Med. Dec 12.2012 4:164fs44.
18. Gounaris E, et al. T-regulatory cells shift from a protective anti-inflammatory to a cancer-promoting proinflammatory phenotype in polyposis. Cancer Res. Jul 1.2009 69:5490. [PubMed: 19570783]
19. Colombo MP, Piconese S. Polyps wrap mast cells and Treg within tumorigenic tentacles. Cancer Res. Jul 15.2009 69:5619. [PubMed: 19567669]
20. Kinzler KW, Vogelstein B. Lessons from hereditary colorectal cancer. Cell. Oct 18.1996 87:159. [PubMed: 8861899]
21. Harada N, et al. Intestinal polyposis in mice with a dominant stable mutation of the beta-catenin gene. Embo J. 1999; 18:5931. [PubMed: 10545105]
22. Gounaris E, et al. Mast cells are an essential hematopoietic component for polyp development. Proc Natl Acad Sci U S A. Dec 11.2007 104:19977. [PubMed: 18077429]

23. Harada N, et al. Intestinal polyposis in mice with a dominant stable mutation of the beta-catenin gene. The EMBO journal. Nov 1.1999 18:5931. [PubMed: 10545105]
24. Dennis KL, et al. Adenomatous polyps are driven by microbe-instigated focal inflammation and are controlled by IL-10 producing T-cells. Cancer Research. 2013 in press.
25. Germar K, et al. T-cell factor 1 is a gatekeeper for T-cell specification in response to Notch signaling. Proc Natl Acad Sci U S A. Dec 13.2011 108:20060. [PubMed: 22109558]
26. Kovalovsky D, et al. Beta-catenin/Tcf determines the outcome of thymic selection in response to alphabetaTCR signaling. J Immunol. Sep 15.2009 183:3873. [PubMed: 19717519]
27. Guo Z, et al. Beta-catenin stabilization stalls the transition from double-positive to single-positive stage and predisposes thymocytes to malignant transformation. Blood. Jun 15.2007 109:5463. [PubMed: 17317856]
28. Yu Q, Sen JM. Beta-catenin regulates positive selection of thymocytes but not lineage commitment. J Immunol. Apr 15.2007 178:5028. [PubMed: 17404285]
29. Xu Y, Banerjee D, Huelsken J, Birchmeier W, Sen JM. Deletion of beta-catenin impairs T cell development. Nat Immunol. Dec.2003 4:1177. [PubMed: 14608382]
30. Gounari F, et al. Somatic activation of beta-catenin bypasses pre-TCR signaling and TCR selection in thymocyte development. Nat Immunol. Sep.2001 2:863. [PubMed: 11526403]
31. Wang R, et al. T cell factor 1 regulates thymocyte survival via a RORgammat-dependent pathway. Journal of immunology. Dec 1.2011 187:5964.
32. Ding Y, Shen S, Lino AC, Curotto de Lafaille MA, Lafaille JJ. Beta-catenin stabilization extends regulatory T cell survival and induces anergy in nonregulatory T cells. Nat Med. Feb.2008 14:162. [PubMed: 18246080]
33. van Loosdregt J, et al. Canonical wnt signaling negatively modulates regulatory T cell function. Immunity. Aug 22.2013 39:298. [PubMed: 23954131]
34. Muranski P, et al. Th17 cells are long lived and retain a stem cell-like molecular signature. Immunity. Dec 23.2011 35:972. [PubMed: 22177921]
35. Yu Q, Sharma A, Ghosh A, Sen JM. T cell factor-1 negatively regulates expression of IL-17 family of cytokines and protects mice from experimental autoimmune encephalomyelitis. Journal of immunology. Apr 1.2011 186:3946.
36. Ma J, Wang R, Fang X, Ding Y, Sun Z. Critical role of TCF-1 in repression of the IL-17 gene. PLoS ONE. 2011; 6:e24768. [PubMed: 21935461]
37. Gounaris E, et al. Live imaging of cysteine-cathepsin activity reveals dynamics of focal inflammation, angiogenesis, and polyp growth. PLoS One. 2008; 3:e2916. [PubMed: 18698347]
38. Khazaie K, et al. Abating colon cancer polyposis by Lactobacillus acidophilus deficient in lipoteichoic acid. Proceedings of the National Academy of Sciences of the United States of America. Jun 26.2012 109:10462. [PubMed: 22689992]
39. Gounari F, et al. Loss of adenomatous polyposis coli gene function disrupts thymic development. Nat Immunol. Aug.2005 6:800. [PubMed: 16025118]
40. Khazaie K, et al. Abating colon cancer polyposis by Lactobacillus acidophilus deficient in lipoteichoic acid. Proc Natl Acad Sci U S A. Jun 26.2012 109:10462. [PubMed: 22689992]
41. Saam JR, Gordon JI. Inducible gene knockouts in the small intestinal and colonic epithelium. J Biol Chem. Dec 31.1999 274:38071. [PubMed: 10608876]
42. Lee PP, et al. A critical role for Dnmt1 and DNA methylation in T cell development, function, and survival. Immunity. Nov.2001 15:763. [PubMed: 11728338]
43. Mottet C, Uhlig HH, Powrie F. Cutting edge: cure of colitis by CD4+CD25+ regulatory T cells. J Immunol. Apr 15.2003 170:3939. [PubMed: 12682220]
44. Blatner NR, et al. In colorectal cancer mast cells contribute to systemic regulatory T-cell dysfunction. Proceedings of the National Academy of Sciences of the United States of America. Apr 6.2010 107:6430. [PubMed: 20308560]
45. Mosimann C, Hausmann G, Basler K. Beta-catenin hits chromatin: regulation of Wnt target gene activation. Nature reviews Molecular cell biology. Apr.2009 10:276.
46. Eberl G, et al. An essential function for the nuclear receptor RORgamma(t) in the generation of fetal lymphoid tissue inducer cells. Nat Immunol. Jan.2004 5:64. [PubMed: 14691482]

47. Parker DS, Ni YY, Chang JL, Li J, Cadigan KM. Wingless signaling induces widespread chromatin remodeling of target loci. Mol Cell Biol. Mar.2008 28:1815. [PubMed: 18160704]
48. Samstein RM, et al. Foxp3 exploits a pre-existent enhancer landscape for regulatory T cell lineage specification. Cell. Sep 28.2012 151:153. [PubMed: 23021222]
49. Otero K, et al. Macrophage colony-stimulating factor induces the proliferation and survival of macrophages via a pathway involving DAP12 and beta-catenin. Nat Immunol. Jul.2009 10:734. [PubMed: 19503107]
50. Wood LD, et al. The genomic landscapes of human breast and colorectal cancers. Science. Nov 16.2007 318:1108. [PubMed: 17932254]
51. Kim G, Levin M, Schoenberger SP, Sharpe A, Kronenberg M. Paradoxical effect of reduced costimulation in T cell-mediated colitis. J Immunol. May 1.2007 178:5563. [PubMed: 17442938]
52. Zhang J, et al. Harnessing of the nucleosome-remodeling-deacetylase complex controls lymphocyte development and prevents leukemogenesis. Nat Immunol. Jan.2012 13:86. [PubMed: 22080921]
53. Hattori N, Kawamoto H, Fujimoto S, Kuno K, Katsura Y. Involvement of transcription factors TCF-1 and GATA-3 in the initiation of the earliest step of T cell development in the thymus. J Exp Med. Sep 1.1996 184:1137. [PubMed: 9064330]
54. Langmead B, Trapnell C, Pop M, Salzberg SL. Ultrafast and memory-efficient alignment of short DNA sequences to the human genome. Genome biology. 2009; 10:R25. [PubMed: 19261174]
55. Zhang B, et al. The prevalence of Th17 cells in patients with gastric cancer. Biochemical and biophysical research communications. Sep 26.2008 374:533. [PubMed: 18655770]

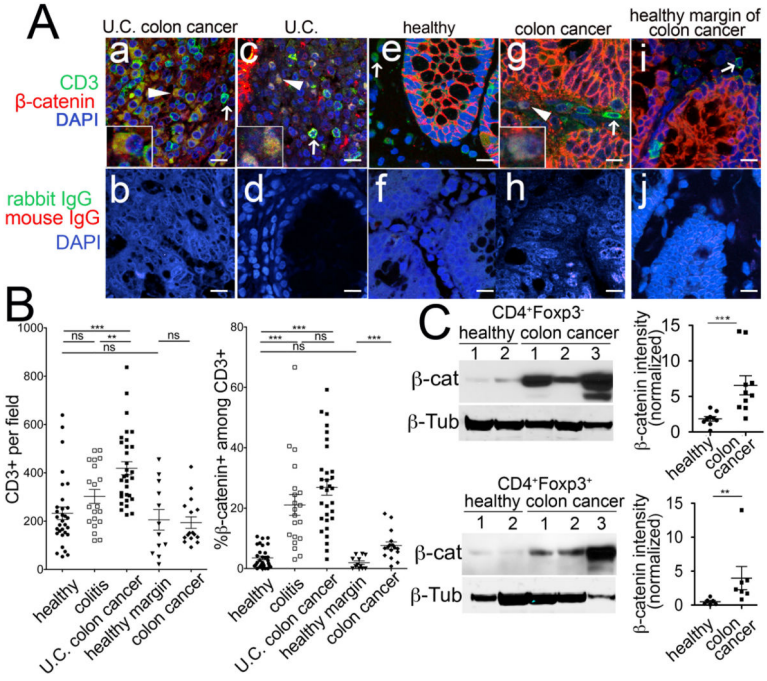

Fig 1. β-catenin is upregulated in T-cells and Tregs of colon cancer patients

A. Representative images for CD3 (green), β-catenin (red), and DAPI (blue) or isotype controls rabbit IgG (green), mouse IgG1 (red), and DAPI (blue) immunofluorescence, imaged by confocal microscopy (Leica; 1000X magnification). Immunostaining of CD3, β-Catenin, and DAPI is depicted for (a) Ulcerative Colitis (U.C.) associated colon cancer, (c) Colitis, (e) Healthy, (g) Sporadic colon cancer, and (i) Healthy Margin of Sporadic colon cancer. Also, Immunostaining for Isotype controls are depicted for (b) U.C. Associated colon cancer, (d) Colitis, (f) Healthy, (h) Sporadic colon cancer, and (j) Healthy Margin of Sporadic colon cancer. Arrowheads show $CD3^+$ β-$catenin^+$ T cells, and arrows depict $CD3^+$ β-$catenin^-$ T cells. **B.** Quantification of infiltration of colon by $CD3^+$ and β-$catenin^+CD3^+$ T cells in "healthy" individuals (n=7) (patients with AVM or diverticular disease) or "colitis" patients (n=5) or "U.C. colon cancer tumors" (n=4), "healthy margin" of sporadic colon cancer (n=)and sporadic "colon cancer" tumors. 4–6 independent fields per patient were quantified. ***P<0.0001, **P<0.006, Student's two-tailed T-test. **C.** Western-blot analysis of purified $CD4^+Foxp3^-$ and $CD4^+Foxp3^+$ T-cells from colon cancer patients normalized for β-tubulin. Each sign represents one patient. *P<0.02, two-tailed T-test. Each well contains whole cell lysates from 4×10^5 cells.

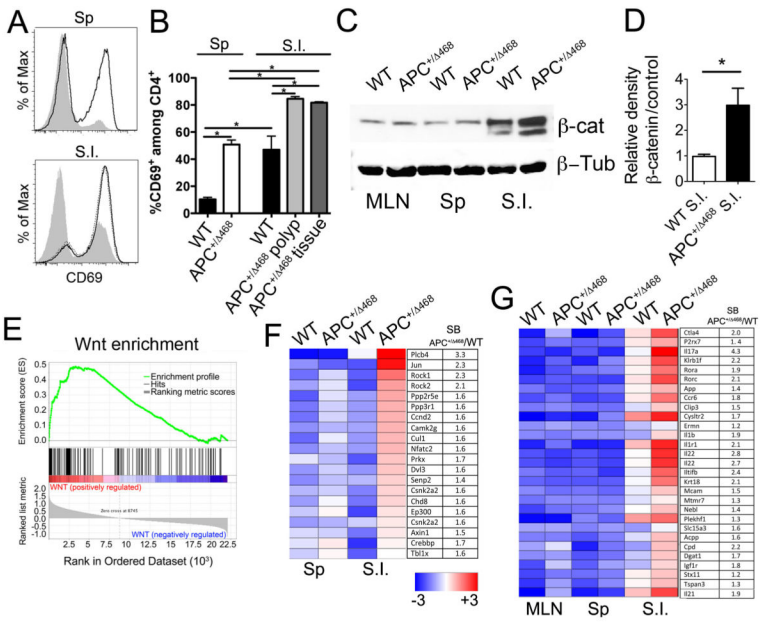

Fig 2. Upregulation of activation markers and β-Catenin, Wnt, and TH17 genes in CD4 T-cells during polyposis

A. Histogram overlays show surface expression of CD69 by WT (gray) and APC$^{+/\Delta 468}$ (clear) CD4^{+} T-cells from mouse spleen (Sp) and small intestine (S.I.). **B.** Frequency of CD69^{+}CD4^{+} T-cells from indicated tissues and mice (n=5); *p<0.05. **C.** Representative β-catenin Western blot of lysates of sorted CD4^{+} T-cells from WT and APC$^{+/\Delta 468}$ mice (MLN: mesenteric lymph nodes). β-Tubulin was probed as loading control. **D.** Histogram bars show quantification of β-catenin protein levels as revealed by WB of CD4^{+} cells from the S.I. as indicated. **E.** GSEA of Wnt pathway genes (Biocarta) in S.I. APC$^{+/\Delta 468}$ compared to WT CD4^{+} T-cells (p=<0.001). **F.** Heatmap showing expression of Wnt pathway genes that are upregulated in APC$^{+/\Delta 468}$ compared to WT S.I. CD4^{+} T-cells. **G.** Heatmap of Affymetrix array data depicting the expression of TH17 signature genes in WT and APC$^{+/\Delta 468}$ CD4^{+} T-cells. Each square represents the average of 3–5 values. Gene IDs and fold change in expression in APC$^{+/\Delta 468}$ versus WT CD4^{+} T-cells are shown. For WB and microarray experiments, samples were magnetically enriched for CD4^{+} T-cells and then twice sorted to >97% purity (See Fig S1 A).

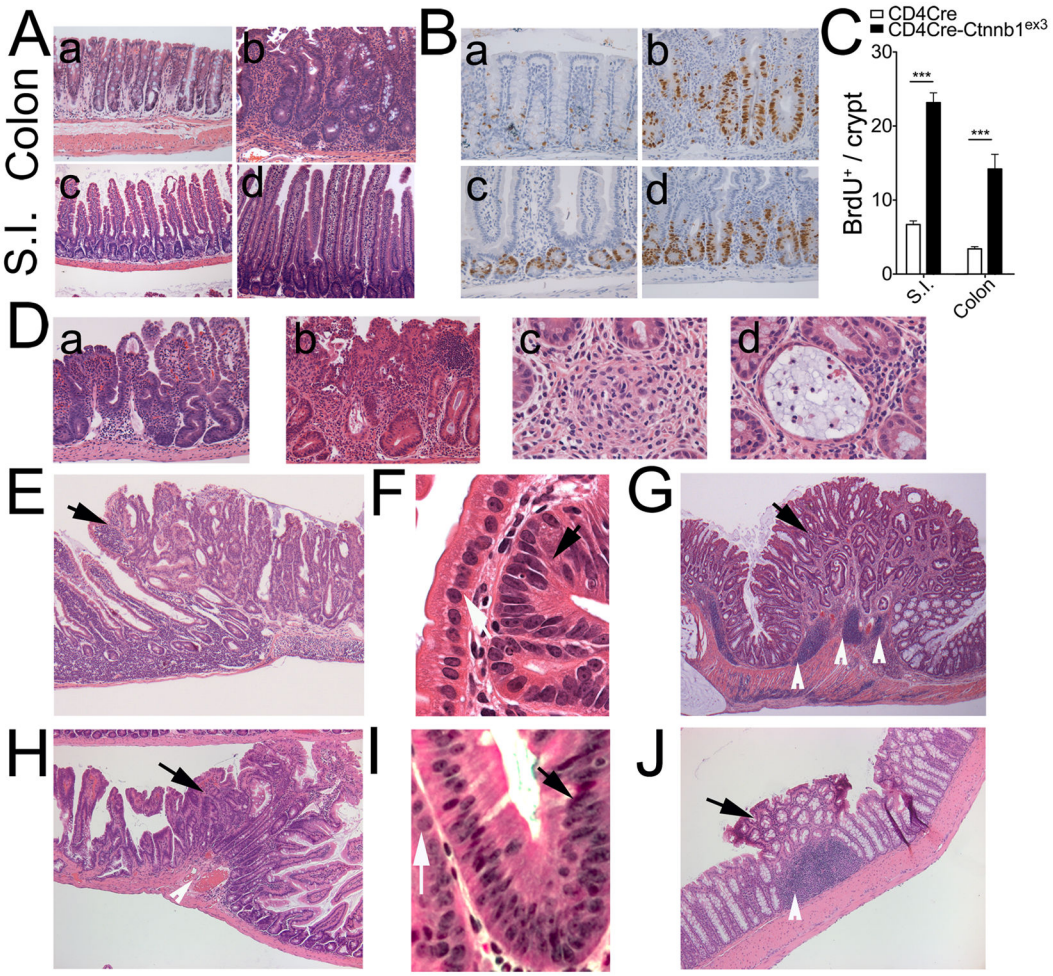

Fig 3. Intestinal pathologies in CD4CreCtnnb^{ex3} mice

A. Stabilization of β-catenin in T-cells causes inflammation. Crypt and villi elongation in CD4CreCtnnb^{ex3} colon (a) and S.I. (c) compared to WT (b) and (d), respectively. **B.** Increased mitosis of intestinal epithelial cells. BrdU staining with hematoxylin counterstain: (a) WT colon, (b) CD4CreCtnnb^{ex3} colon, (c) WT S.I., (d) CD4CreCtnnb^{ex3} S.I. **C.** Histograms showing quantification of epithelial mitotic activity (BrdU staining) in S.I and colon of wt and CD4CreCtnnb^{ex3} mice. Values represent the average count of dividing cells in 10 independent fields. **D.** Representative images of ulcers (a and b), granulomas (c) and crypt abscesses (d) in CD4CreCtnnb^{ex3} intestine. **E. and H.** Small intestine polyp and surrounding tissue in CD4CreCtnnb^{ex3} and Foxp3CreCtnnb^{ex3} mice respectively as indicated (H&E). Black arrows indicate the polyp. **F. and I.** Detail of inflamed crypt in CD4CreCtnnb^{ex3} and Foxp3CreCtnnb^{ex3} mice respectively. Black arrow indicates abnormal nucleus and white arrow indicates normal nucleus **G. and J.** Colonic polyp and surrounding tissue in CD4CreCtnnb^{ex3} and Foxp3CreCtnnb^{ex3} mice (H&E). Black arrow indicates the polyp and white arrows indicate enlarged lymphoid structures.

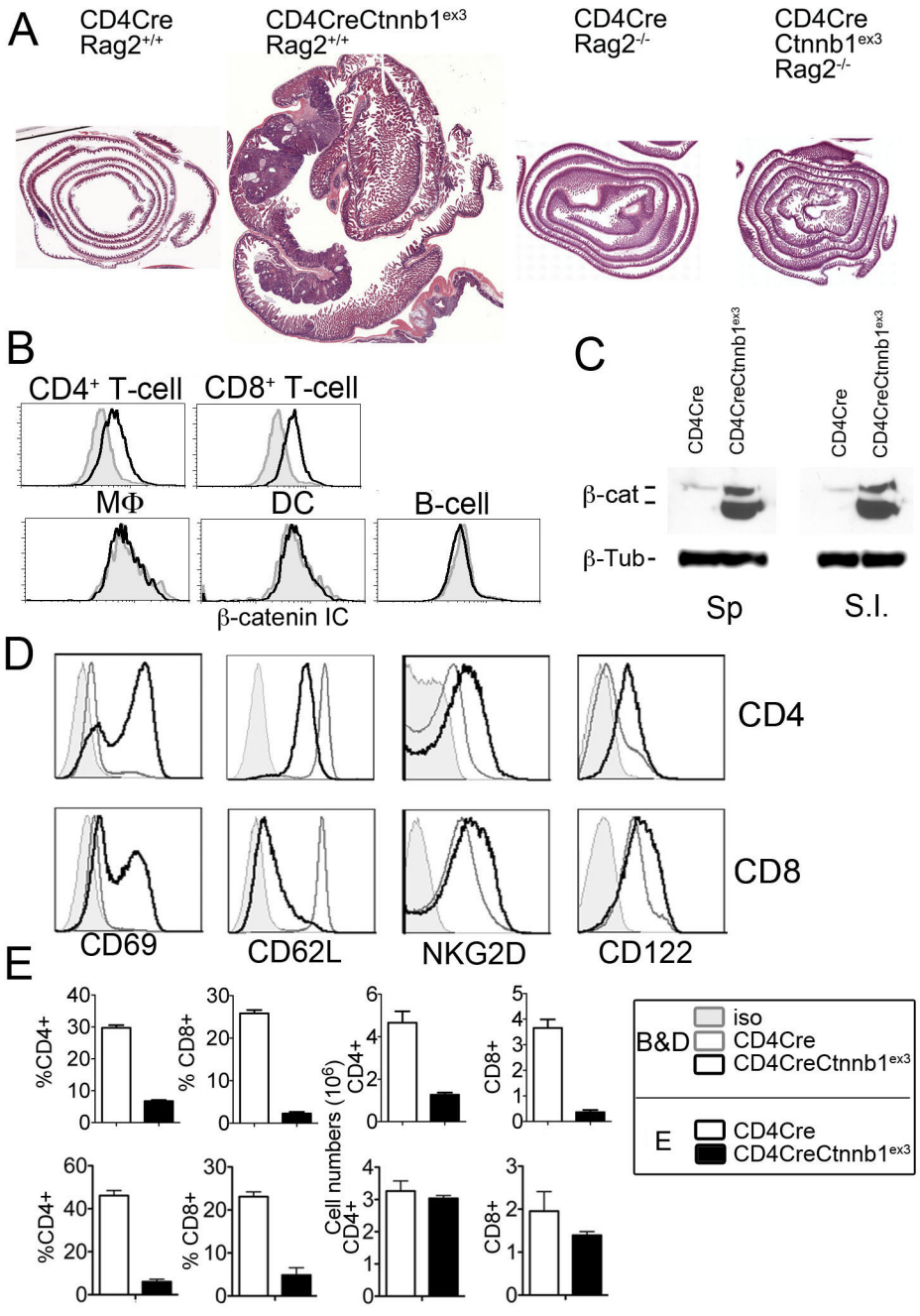

Fig 4. Inflammation and polyposis is induced by stabilization of β-catenin in T-cells

A. Gut dysplasia in CD4CreCtnnb^{ex3} mice is T-cell dependent; HE stained sections of gut rolls from the indicated age matched mice (n=10). Note that no polyps developed in CD4CreCtnnb^{ex3}-Rag2$^{-/-}$ mice. Images are in scale. **B.** Histogram overlays showing intracellular (IC) β-catenin staining in MLN cell suspensions from WT (filled gray) and CD4CreCtnnb1^{ex3} (black line) mice gated for the indicated lineages. Results are representative of more than three independent experiments. **C.** WB of lysates of sorted CD4^{+} T-cells in the indicated tissues of WT and CD4CreCtnnb1^{ex3} mice. β-Tubulin was

probed as loading control. Results are representative of two independent experiments. **D.** Histogram overlays comparing surface expression of activation markers (CD69, NKG2D, and CD122) and naïve cell marker CD62L in CD4 and CD8 MNL cells from WT and CD4CreCtnnb^{ex3} mice. **E.** Upper histograms show frequencies and cell numbers of CD4^{+} and CD8^{+} cells from WT and CD4CreCtnnb^{ex3} MLN as indicated, prior to the onset of inflammation (4 weeks of age) (n=3–8). Lower histograms show frequencies and cell numbers of CD4^{+} and CD8^{+} cells from WT and CD4CreCtnnb^{ex3} MLN as indicated, after onset of inflammation (8–10 weeks of age) (n=3–8).

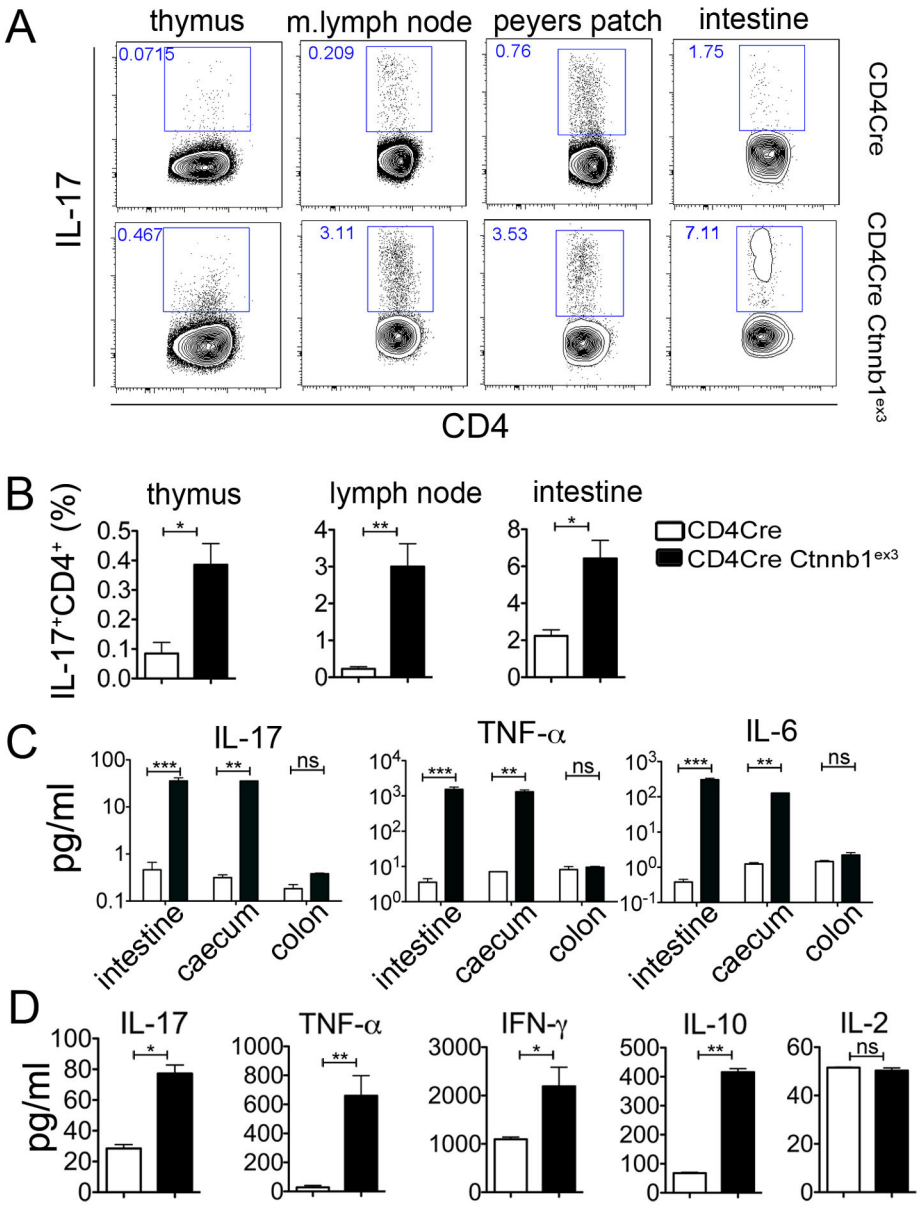

Fig 5. Enhanced levels of proinflammatory cytokines in CD4CreCtnnb^{ex3} mice

A. Dot plots showing frequencies of IL17 expressing CD4 T-cells in the indicated organs from wt and CD4CreCtnnb^{ex3} mice. Note increased frequency of IL17 expressing CD4^{+} cells starts in SP thymocytes. **B.** Histograms showing the frequency of IL17 expressing CD4^{+} T-cells in the indicated organs from WT and CD4CreCtnnb^{ex3} mice (n=3–8). **C.** Histograms showing quantification of the concentration of the indicated cytokines in lysates from the indicated parts of the intestine of WT versus CD4CreCtnnb^{ex3} mice (n=3). Results are representative of two independent experiments. **D.** Histograms showing concentrations of the indicated cytokines in the serum of recipient Rag2$^{-/-}$ mice injected with 10^{6} T-cells isolated from WT or CD4CreCtnnb^{ex3} mice four weeks after transfer (n=3). Results are representative of two independent experiments.

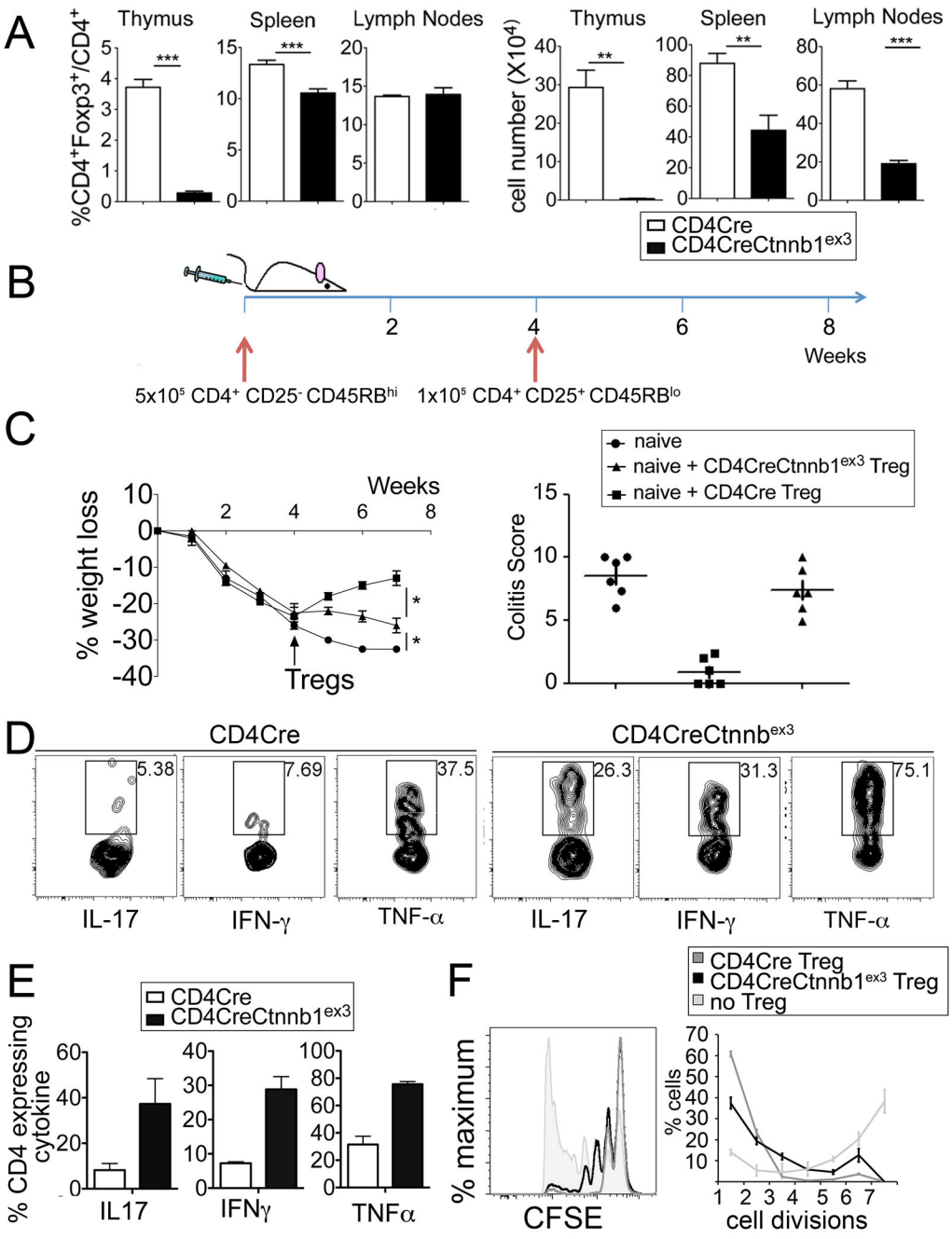

Fig 6. Development and function of Tregs with constitutively active β-catenin

A. Frequency and number of $CD4^+Foxp3^+$ among $CD4^+$ T-cells in the indicated organs and mice (n>3). $CD4CreCtnnb1^{ex3}$ and littermate-control mice were analyzed at 4 weeks of age prior to the onset of inflammation. **B.** Scheme of *in vivo* colitis induction in $Rag2^{-/-}$ mice to assess the anti-inflammatory properties of Tregs. Arrows indicate adoptive transfer of the indicated sorted cell populations **C.** (left) Percent loss of starting weight over time. Tregs were injected 4 weeks after injection of naïve T-cells. (right) Colitis-score was calculated based on percent colon involvement, severity of inflammation, level of involvement, and

extent of damage. **D.** Contour-plots showing expression of the indicated pro-inflammatory cytokines in $CD45.2^{+}CD4^{+}Foxp3^{+}$ donor Tregs retrieved from the gut of $Rag2^{-/-}$ recipients at endpoint. **E.** Histograms showing the average frequencies of cytokine expression shown in **D** (n=5). **F.** *In vitro* proliferation inhibition. CFSE labeled naive WT T-cells were stimulated with IL2 and anti-CD3 and anti-CD28, and then plated at a 1:2 ratio with CD4Cre or $CD4CreCtnnb^{ex3}$ Tregs. Proliferation was assessed by CFSE dilution. Filled histogram shows proliferation of activated T-cells in the absence of Tregs. Note that $CD4CreCtnnb1^{ex3}$ Tregs only partially inhibit proliferation of activated T-cells as compared to WT Tregs.

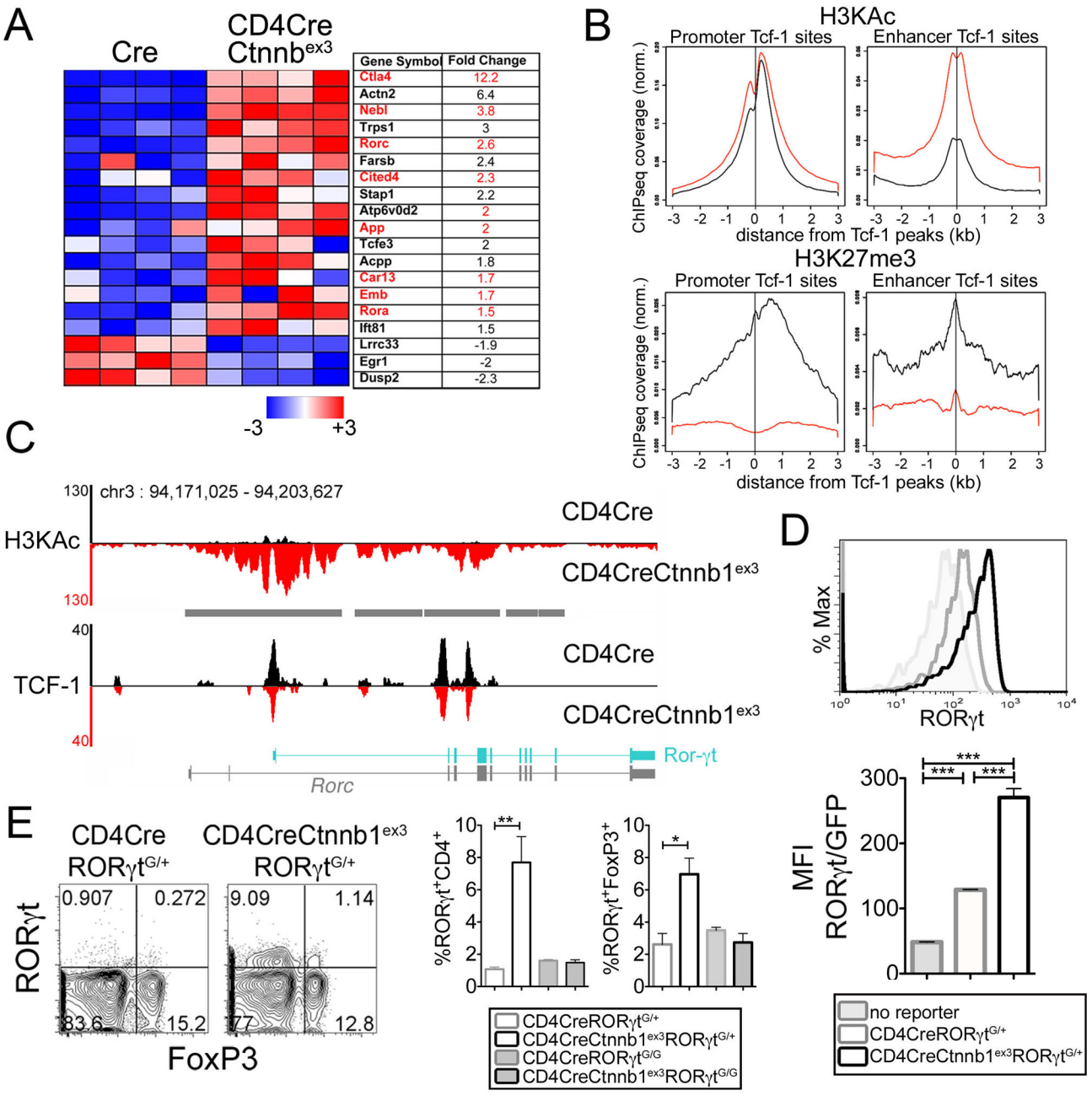

Fig 7. β-catenin stabilization induces sustained RORγt expression in T-cells and Tregs

A. Heatmap depicts significant expression changes in TH17-lineage genes induced by β-catenin stabilization in CD4CreCtnnb1^{ex3} DP-thymocytes. Columns represent independent arrays for the indicated mouse strain. Gene IDs and average fold expression change are shown. Red letters depict genes similarly changed in gut CD4 T-cells during polyposis (Fig 1G). **B.** Histograms illustrate normalized average-tag-density distribution of the indicated histone marks in CD4Cre (black) and CD4CreCtnnb1^{ex3} (red) DP-thymocytes centered on shared Tcf-1 peaks. Tcf-1 binding at sites <3 kb or >3 kb from the nearest transcription start site are considered promoter or enhancer binding, respectively. **C.** Peaks of Tcf-1 binding

and H3KAc marks in the Rorc locus of CD4Cre and CD4CreCtnnb1^{ex3} thymocytes. Diagrams depict the Rorc locus. RORγt is in cyan. Gray bars indicate >3 fold increases in H3KAc marks. **D.** Histogram-overlays showing expression levels of RORγt-GFP reporter in gated CD4 SP, and histogram-bars showing average mean-fluorescence-intensity (MFI) of RORγt-GFP expression (n=5) in the indicated mouse strains. **E.** Contour-plots of intracellular Foxp3/RORγt staining in gated CD4$^+$ splenic T-cells from the indicated mouse strains. **F.** Frequency of RORγt$^+$ cells among CD4$^+$ or CD4$^+$Foxp3$^+$ splenocytes as indicated (n=3); **p<0.001, *p<0.05. Representative of two independent experiments.

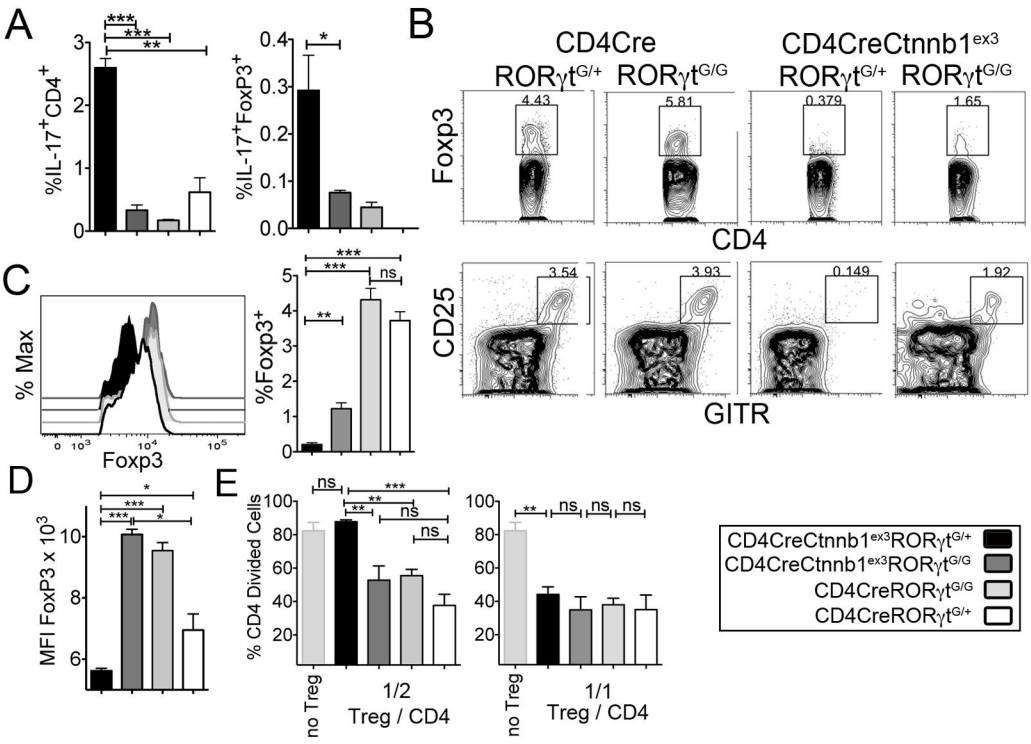

Fig 8. β-catenin mediated upregulation of RORγt affects the development and function of Tregs

A. Histograms showing the percent Foxp3$^+$ cells in gated CD4$^+$ thymocytes of the indicated mice (n=3). Data are representative of two independent experiments. **B.** CD4/Foxp3 (upper) and CD25/GITR (lower) dot plots gated on CD4 SP thymocytes of the indicated mouse strains. **C.** Histogram overlay showing intracellular Foxp3 staining in CD4$^+$Foxp3$^+$ splenic T-cells, and histogram bars showing cumulative Foxp3 mean fluorescence intensity (MFI) in the indicated mouse strains (n=3). Note the comparable increase in Foxp3 levels upon RORγt ablation both in Tregs with physiological β-catenin levels and in Tregs with stabilized β-catenin. **D.** Histograms showing the frequency (%) of IL17$^+$CD4$^+$ cells (left) and IL17$^+$Foxp4$^+$ Tregs in the spleen of the indicated mice (n=3). Data are representative of two independent experiments. **E.** Histogram bars showing the fraction of proliferating CFSE labeled T effector cells (CD4) cultured at a 1:2 or 1:1 ratio (Treg:T effector) in the presence of Tregs isolated from the indicated mice. Note that ablation of RORγt in Tregs with stabilized β-catenin significantly enhances their ability to inhibit proliferation of activated CD4 T-cells. B-E: ***p<0.0001, **p<0.001, *p<0.05.